

*Short Communication*

## **Wheat shell biomass-derived carbon materials for superior polysulfide adsorption and energy storage**

*Tao Ding*

Department of Mechanical and Electrical Engineering, Yongcheng Vocational College, Yongcheng, 476600, China.

E-mail: [taodinyvc@126.com](mailto:taodinyvc@126.com)

*Received: 5 December 2021 / Accepted: 17 January 2022 / Published: 4 March 2022*

Lithium-sulfur batteries have high specific capacity and energy density, which is much higher than the traditional lithium-ion batteries. Therefore, it could replace the LIBs in the market for the electric vehicles. However, there are still problems to hinder the wide application of the lithium-sulfur batteries. The main issues are including the insulation of the element sulfur and the dissolution of the soluble polysulfide during the discharging and charging process. For overcoming these problems, many works have been conducted, such as preparing the advanced S-based cathode materials, designing the multifunctional separators and interlayers between the cathode and lithium anode. Herein, wheat biomass-derived carbon materials were prepared and used as sulfur host materials in the lithium-sulfur batteries. Owing to high electronic conductivity as well as abundant active site of carbon materials, the as-prepared carbon/S composites could accelerate the polysulfide conversion and the electrode reaction kinetics. As a result, the as-prepared carbon/S composites exhibit superior rate performance and outstanding cycling stability as cathode materials during the electrochemical cycles.

**Keywords:** Sulfur host; Carbon; Conversion; Lithium-sulfur battery; Polysulfide.

### **1. INTRODUCTION**

Lithium-sulfur batteries have been considered as the most promising energy storage system due to their high specific capacity (1675 mAh/g) and energy density (2600 Wh/Kg) [1, 2]. In addition, the element sulfur has advantages of abundant resource, non-toxic and environmental friendless [3, 4, 5]. However, some shortcomings, especially the polysulfide migration and poor electronic conductivity hindered the wide practical application of the lithium-sulfur batteries [6-9]. Given these problems, many strategies have been applied to solve the above issues [10, 11]. Therefore, many attempts have been paid on the employment of the suitable sulfur host materials and multifunctional separators and interlayers between the cathode and lithium anode, which could improve the electrochemical

performance of the lithium-sulfur batteries [12-15].

Among various methods, preparing the advanced S-based cathode materials has been viewed as the most promising strategy to modify the electrochemical performance of the lithium-sulfur batteries [16]. During the past decades, much works have been reported to improve the electrochemical performance [17]. Yan et al reported organosulfur copolymers as the cathode materials for the lithium-sulfur batteries [18]. Due to the rapid lithium-ion diffusivity, the as-prepared organosulfur copolymers show excellent electrochemical performance [19]. Besides, the carbon materials were also designed as sulfur host materials in the lithium-sulfur batteries. The main carbon materials are including carbon nanofiber, carbon nanotube, graphene and other carbon-based materials [20, 21, 22]. However, so far, there are few works about the biomass carbon materials in the lithium-sulfur batteries.

In this work, we prepared carbon materials via wheat biomass and the as-prepared carbon materials were used as sulfur host materials in the lithium-sulfur batteries. Owing to high electronic conductivity as well as abundant active site of carbon materials, the as-prepared carbon/S composites could accelerate the polysulfide conversion and the electrode reaction kinetics. Therefore, the electronic conductivity and polysulfide migration could be improved and inhibited, respectively. As a result, the as-prepared carbon/S composites exhibit superior rate performance and outstanding cycling stability as cathode materials during the electrochemical cycles. The initial specific capacity of the carbon/S composite is as high as 1295 mAh/g at 0.1 C. The excellent electrochemical performance is attributed to the presence of the carbon materials, which could enhance the electron transport and inhibit the polysulfide shuttle effect at the same time.

## 2. EXPERIMENTAL

### 2.1. Preparation of the carbon/S composite

All chemicals used in this work were analytical pure without any further purification and commercially available. Deionized water used was house generated.

Wheat shell was pyrolyzed at 800 °C for 3 h with a heating rate of 5 °C min<sup>-1</sup> to obtain derived carbon. Then, the carbon was subjected to KOH solution to obtain activated carbon. In detail, 2.1 g carbon and 2.5 g KOH were mixed in 60 mL deionized water for 12 h. The sample was dried at 80 °C overnight and collected for pyrolysis at 600 °C for 3 h at 2 °C min<sup>-1</sup>. Finally, the carbon/S composites were prepared by heating the carbon and sulfur mixture at 155 °C for 15 h.

### 2.2. Materials Characterization

X-ray diffraction (XRD) measurements were performed to verify the crystalline structures using Cu K $\alpha$  radiation ( $k = 1.5418 \text{ \AA}$ ) at a scanning rate of 2° min<sup>-1</sup> in the 2 $\theta$  range of 10°-80°. Thermogravimetric analysis (TGA, Netzsch) was used to detect the amount of sulfur at a heating rate of 10 °C min<sup>-1</sup> under air atmosphere. Scanning electron microscopy (SEM) and transmission electron

microscope (TEM) were measured to study the morphologies. X-ray photoemission spectroscopy (XPS) was carried out to study the chemical valence in the samples. Raman spectra were tested by Renishaw inVa using a laser with an excitation wavelength of 532 nm.

### 2.3. Electrochemical performance

CR-2032 coin batteries were assembled in an argon-filled glove box. The cathode slurry was prepared by mixing 80 % active materials, 10% carbon black and 10% PVDF in NMP. Then, the slurry was uniformly coated on the Al film and dried at 60 °C for 24h. The lithium foil was used as counter and anode. The Celgard 2500 film was used as separator between the cathode and lithium anode. 1 M lithium bis-(trifluoromethanesulfonyl) imide dissolved in 1, 2-dimethoxyethane and 1, 3-dioxolane (DME: DOL=1:1 volume ratio) with 0.1 M LiNO<sub>3</sub> was used as the electrolyte. The galvanostatic charge-discharge measurements of the coin cells were carried out using Land CT2001A between 1.7-2.8 V. Cyclic voltammetry (CV) and electrochemical impedance spectroscopy (EIS) were measured by CHI660E electrochemical workstation.

## 3. RESULTS AND DISCUSSION

**Fig. 1a** shows the N<sub>2</sub> adsorption and desorption curves of the carbon and carbon/S composites. As it can be seen that the as-prepared carbon materials have abundant pores with mesoporous structure, the carbon materials is beneficial for the employment of the sulfur host in the lithium-sulfur batteries. After sulfur loading (red curve), it can be seen that the as-prepared carbon/S composites have no mesoporous structure. This is attributed to the occupation of the element sulfur into the mesopores of the carbon hosts materials. Besides, the specific surface area of the carbon/S composites decreased after the element sulfur loading, confirming the successful preparation of the carbon/S composites. Moreover, XRD patterns of the samples were tested to identify the crystal structure. As shown in **Fig.1b**, the as-prepared carbon materials show amorphous structure with a wide peak at 25°, which is related to the (001) plane of the carbon materials [23]. After loading the element sulfur, the as-prepared carbon/S composites exhibit the typical diffraction peaks of the element sulfur, indicating the preparation of the carbon/S composites.

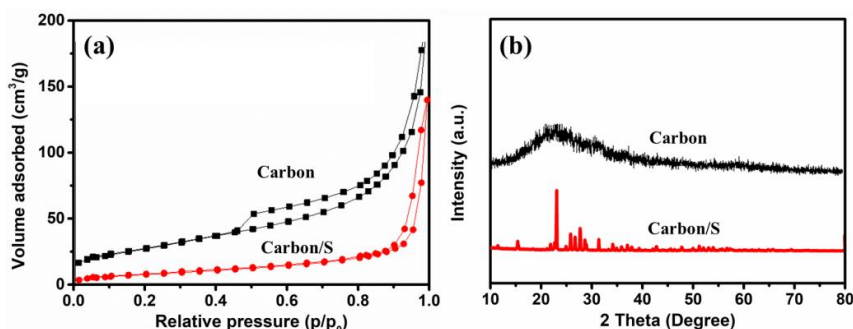


**Figure 1.** (a) N<sub>2</sub> adsorption and desorption profiles of the carbon and carbon/S composites. (b) XRD patterns of the carbon and carbon/S composites at 2θ range of 10°-80°.

**Fig. 2a** shows the preparing process for the carbon/S composites. As depicted in Fig. 2a, firstly, the collected wheat shells are pyrolyzed at 800 °C for 3 h with a heating rate of 5 °C min<sup>-1</sup> to obtain derived carbon. Then, the carbon was subjected to KOH solution to obtain activated carbon. In detail, 2.1 g carbon and 2.5 g KOH were mixed in 60 mL deionized water for 12 h. The sample was dried at 80 °C overnight and collected for pyrolysis at 600 °C for 3 h at 2 °C min<sup>-1</sup>. As a result, the active carbon samples were successfully prepared. The active carbon has large specific surface and sufficient active sites, which have been confirmed in **Fig. 1a**. Finally, the active carbon/S composites were prepared by heating the carbon and sulfur mixture at 155 °C for 15 h. During the heating period, the element sulfur could be fully immersed into the mesoporous structure of the active carbon materials. The carbon/S composites were used to prepare the electrode slurry for the LSB. To observe the morphology of the samples, scanning electron microscopy was tested for the carbon/S composites. As shown in **Fig. 2b**, it can be seen that the element sulfur particles are uniformly immersed into the active carbon materials, demonstrating the uniform dispersion of element sulfur in the active carbon materials. Furthermore, the TEM image of the sample was collected. As shown in **Fig. 2c**, the shadow indicates the dispersion of the elements sulfur particles in the carbon/S composites.

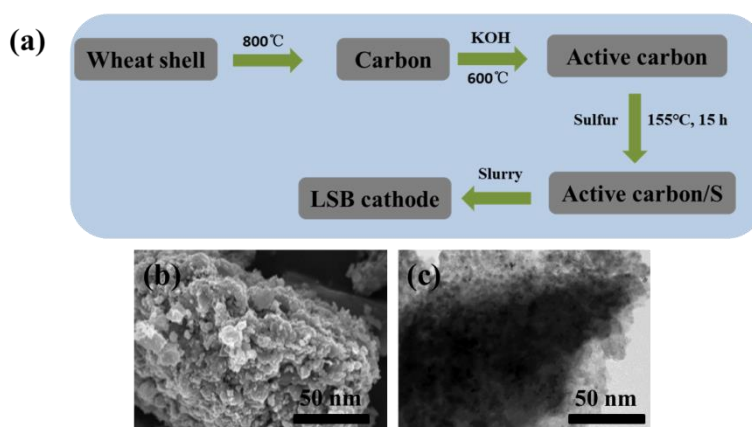


**Figure 2.** (a) Preparing process of the carbon/S composites. (b) and (c) SEM and TEM image of the carbon/S composites.

To investigate the chemical valence in the as-prepared carbon/S composites, XPS was conducted for the carbon/S composites. As shown in **Fig. 3a**, for the S 2p, there are two peaks at 164.3 eV and 165.8 eV, which are corresponding to the S 2p<sub>3/2</sub> and S2p<sub>1/2</sub>, respectively [24]. This confirms the successful immersion of the element sulfur into the mesoporous structure of the carbon materials. In addition, **Fig. 3b** shows the XPS spectrum of the C 1s. It can be seen that there are two main peaks at 283.9 eV and 289.1 eV, which are related to the C-C chemical bond and C-C=O bond, respectively [25]. More importantly, there is one peak at 285.6 eV. This represents the chemical bond C-S between the carbon materials and sulfur, confirming the strong relationship between the carbon host and polysulfide.

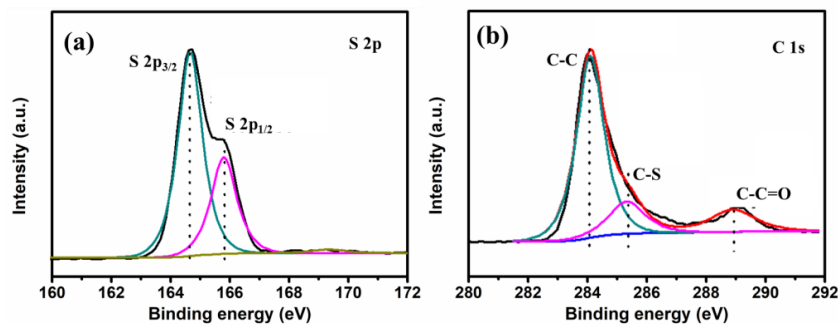


**Figure 3.** XPS spectrum for the carbon/S composite (a) S 2p and (b) C 1s.

The constant discharge and charge profiles of the carbon/S composites were tested between 1.7 V and 2.8 V. As shown in **Fig. 4a**, the capacity of the carbon/S composites is 967 mAh/g after 80 cycles at 0.2 C, which is much higher than the other carbon sulfur host materials in the lithium-sulfur batteries. Besides, it can be seen that the Coulombic efficiency of the carbon/S composite cathode is close to 98%, demonstrating high discharge and charge efficiency. However, the discharge platform at 2.1 V is lean with the increase of the cycle numbers, which is related to the high polarization during the electrochemical cycles. Overall, the high specific capacity of the carbon/S composites is attributed to the high electronic conductivity as well as the abundant active site of carbon materials, which could facilitate the electron transport and adsorb the soluble polysulfide during the discharging and charging process. Electrochemical impedance spectrum was conducted for the carbon/S composite cathode at the different cycles. As shown in **Fig. 4b**, there is one semicircle and a line in the high and low frequency, respectively. They are corresponding to the charge transfer resistance and lithium-ion diffusion in the electrode materials, respectively [26]. The much bigger semicircle in the high frequency region indicate the much higher resistance of the electrode materials. Thus, clearly, the as-prepared carbon/S composite cathode showed no obvious change of the resistance values at the different electrochemical cycles. This further confirms the high electronic conductivity of the carbon/S composite cathode due to the presence of the carbon materials.

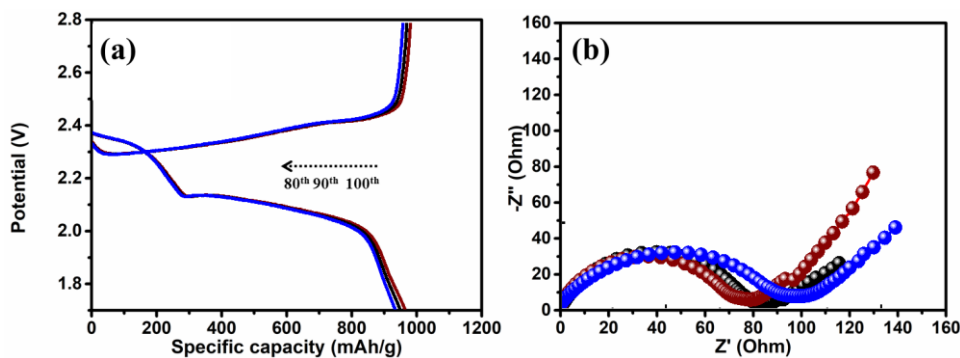


**Figure 4.** (a) The constant discharge and charge profiles of the carbon/S composites at the current density of 0.2 C. (b) Electrochemical impedance spectrum of the carbon/S composite at different cycles.

The cycle performance of the carbon/S composites was tested at the current density of 1 C for 100 cycles. As shown in **Fig. 5a**, the as-prepared carbon/S composites showed initial specific capacity of 986 mAh/g at 1 C, which is much higher than the other S-based composite cathode. This is related to the improvement of the electronic conductivity of the carbon/S composites. In addition, the as-prepared carbon/S composites delivered capacity of 902 mAh/g at 1C after 100 electrochemical cycles. This demonstrates the superior cycling stability of the carbon/S composites, which could enhance the electron transport and inhibit the polysulfide shuttle effect at the same time. **Fig. 5b** shows the CV curves of the carbon/S composites between 1.7 V and 2.8 V. It can be seen that the as-prepared carbon/S composites exhibit two reduction peaks at 2.35 V and 2.12 V. These reduction peaks are related to the electrochemical reaction between the element sulfur and lithium-ion. Moreover, there is one oxidation peak at 2.4 V, which is the reversible electrochemical reaction from  $\text{Li}_2\text{S}$  to element sulfur. All these redox peaks can be matched well with the platforms in the discharging and charging profiles in Figure 4a. Moreover, it can be seen that the CV curves overlap well with the increase of the cycle numbers. This indicates the superior electrode reversibility during the electrochemical cycles, which is ascribed to the superior electrochemical kinetics.

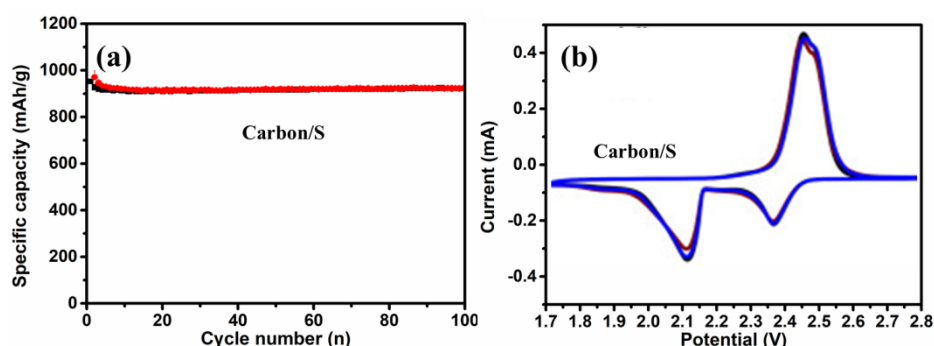


**Figure 5.** (a) Cycle performance of the carbon/S composite at the current density of 1 C. (b) CV curve of the carbon/S composites with scanning rate of  $0.1 \text{ mV s}^{-1}$ .

To further demonstrate the superior electrochemical performance of the carbon/S composite cathode materials, a table was made to compare the electrochemical performance of the cathode materials. As listed in **Table 1**, the electrochemical performance of various cathode materials for LBSs is displayed. It can be seen that the carbon/S cathode materials shows high capacity of 986 mAh/g after 100 cycles at the current density of 1 C, demonstrating the stable cycling performance. However, other similar cathode materials show rapid capacity fading with the increase of the cycle numbers, which is attributed to the severe polysulfide migration during the electrochemical cycles. The stable cycling performance of the carbon/S cathode materials is ascribed to its unique structure, which could improve the whole electronic conductivity. At the same time, the carbon structure could provide sufficient active sites to stabilize the polysulfide.

**Table 1.** The comparison of carbon/S cathode with other similar cathode materials in LSBs.

Electrode	Current density	Capacity (mAh/g)	Ref
rGO@HYC/S	0.2C	921 (100 cycles)	27
TiO <sub>2</sub> /S	1C	580 (300 cycles)	28
NiS <sub>2</sub> /rGO/S	1C	400 (200 cycles)	29
S@h-P	0.2C	465 (100 cycles)	30
Carbon/S	1C	986 (100 cycles)	This work

#### 4. CONCLUSION

In summary, we prepared carbon materials via wheat biomass and the as-prepared carbon materials were used as sulfur host materials in the lithium-sulfur batteries. Owing to high electronic conductivity as well as abundant active site of carbon materials, the as-prepared carbon/S composites could accelerate the polysulfide conversion and the electrode reaction kinetics. Therefore, the electronic conductivity and polysulfide migration could be improved and inhibited, respectively. As a result, the as-prepared carbon/S composites exhibit superior rate performance and outstanding cycling stability as cathode materials during the electrochemical cycles. The initial specific capacity of the carbon/S composite is as high as 1295 mAh/g at 0.1 C. The excellent electrochemical performance is attributed to the presence of the carbon materials, which could enhance the electron transport and inhibit the polysulfide shuttle effect at the same time.

#### References

1. Y. F. Li, M. F. Chen, P. Zeng, H. Liu, H. Yu, Z. G. Luo, Y. Wang, B. B. Chang, X. Y. Wang, *J. Alloys Compd.*, 873 (2021) 159883.
2. J. H. Kim, D. J. Lee, H. G. Jung, Y. K. Sun, J. Hassoun, B. Scrosati, *Adv. Funct. Mater.*, 25 (2013) 1076-1080.
3. S. L. Li, W. J. Zhang, J. D. Liu, Y. R. Zhang, Y. H. Zheng, *Appl. Surf. Sci.*, 563 (2021) 150381.
4. L. W. Yang, Y. Li, Y. Wang, Q. Li, Y. X. Chen, B. H. Zhong, X. D. Guo, Z. G. Wu, Y. X. Liu, G. K. Wang, Y. Song, W. Xiang, Y. J. Zhong, *J. Power Sources*, 501 (2021) 230040.
5. S. Zhao, M. S. Zhang, X. C. Xian, *Ionics*, 26 (2020) 617-625.
6. X. M. Zhang, G. R. Li, Y. G. Zhang, D. Luo, A. P. Yu, X. Wang, Z. W. Chen, *Nano Energy*, 86 (2021) 106094.
7. Y. Lu, S. Gu, J. Guo, K. Rui, C. H. Chen, S. P. Zhang, J. Jin, J. H. Yang, Z. Y. Wen, *ACS Appl. Mater. Interfaces*, 9 (2017) 14878-14888.
8. W. Yan, K. Y. Yan, G. C. Kuang, Z. Jin, *Chem. Eng. J.*, 424 (2021) 130316.
9. S. L. Li, X. Zhang, H. Chen, H. M. Hu, J. D. Liu, Y. R. Zhang, Y. X. Pan, Y. H. Zheng, *Electrochim. Acta*, 364 (2020) 137259.
10. L. W. Lin, M. Qi, Z. T. Bai, S. X. Yan, Z. Y. Sui, B. H. Han, Y. W. Liu, *Appl. Surf. Sci.*, 555 (2021) 149717.
11. N. Xu, T. Qian, X. J. Liu, J. Liu, Y. Chen, C. L. Yan, *Nano Lett.*, 17 (2017) 538-543.
12. C. Ma, Z. F. Zheng, X. F. Jia, X. J. Liu, J. T. Wang, W. M. Qiao, L. C. Ling, *J. Power Sources*, 486 (2021) 229358.

13. Y. Du, R. K. Huang, X. D. Lin, S. Khan, B. N. Zheng, R. W. Fu, *Langmuir*, 36 (2020) 14507-14513.
14. B. Fan, D. K. Zhao, W. Xu, Q. K. Wu, W. Zhou, W. Lei, X. H. Liang, L. G. Li, *Electrochim. Acta*, 383 (2021) 138371.
15. H. K. Zhang, X. R. Lin, J. J. Li, T. L. Han, M. F. Zhu, X. Y. Xu, C. Q. Hu, J. Y. Liu, *J. Alloys Compd.*, 881 (2021) 160629.
16. J. Liu, T. Qian, M. F. Wang, X. J. Liu, N. Xu, Y. Z. You, C. L. Yan, *Nano Lett.*, 17 (2017) 5064-5070.
17. K. F. Liu, H. B. Zhao, D. X. Ye, J. J. Zhang, *Chem. Eng. J.*, 417 (2021) 129309.
18. M. J. Yao, R. Wang, Z. F. Zhao, Y. Liu, Z. Q. Niu, J. Chen, *ACS Nano*, 12 (2018) 12503-12511.
19. J. J. Wang, X. Y. Yue, Z. K. Xie, A. M. Patil, S. Peng, X. G. Hao, A. Abudula, G. Q. Guan, *J. Alloys Compd.*, 874 (2021) 159952.
20. F. D. Han, J. Yue, X. L. Fan, T. Gao, C. Luo, Z. H. Ma, L. M. Suo, C. S. Wang, *Nano Lett.*, 16 (2016) 4521-4527.
21. Y. Chu, X. M. Cui, W. L. Kong, K. Y. Du, L. Zhen, L. Q. Wang, *Chem. Eng. J.*, 427 (2022) 130844.
22. D. W. Rao, S. K. Yang, X. H. Yan, *J. Phys. Chem. C*, 124 (2020) 5565-5573.
23. J. H. Won, M. K. Kim, H. M. Jeong, *Appl. Surf. Sci.*, 547 (2021) 149199.
24. S. Choi, S. Kim, M. Cho, Y. K. Lee, *ACS Appl. Energy Mater.*, 3 (2020) 7825-7831.
25. Z. X. Zhao, R. Pathak, X. M. Wang, Z. W. Yang, H. J. Li, Q. Q. Qiao, *Electrochim. Acta*, 364 (2020) 137117.
26. D. Gueon, J. T. Hwang, S. B. Yang, E. Cho, K. Sohn, D. K. Yang, J. H. Moon, *ACS Nano*, 12 (2018) 226-233.
27. Y. J. Li, Y. R. Cai, Z. Y. Cai, J. H. Xu, G. C. Zhu, W. H. Jin, J. M. Yao, *Electrochim. Acta*, 285 (2018) 317-325.
28. A. Chen, W. F. Liu, H. Hu, T. Chen, B. L. Ling, K. Y. Liu, *J. Power Sources*, 400 (2018) 23-30.
29. Y. Li, J. Chen, Y. F. Zhang, Z. Y. Yum T. Z. Zhang, W. Q. Ge, L. P. Zhang, *J. Alloys Compd.*, 766 (2018) 804-812.
30. C. H. Tsao, C. H. Hsu, J. D. Zhou, C. W. Chin, P. L. Kuo, C. H. Chang, *Electrochim. Acta*, 276 (2018) 111-117.